

presence of this chelating bis(stannylene) unit dominates the relative orientation of the remaining ligands. There are two distinct trends in the Rh-Sn bond distances. First, one can observe the expected longer metal-metal bonds of four-coordinate vs three-coordinate tin. Second, the rhodium-tin bond distances of the equatorial ligands are shorter than those of the axial stannylenes. This latter feature is in line with the general trends observed in a number of related trigonal-bipyramidal d^8 systems.¹³ Compounds containing rhodium-tin bonds have been known for only 25 years;¹⁶ few of these have been X-ray structurally characterized. To our knowledge, no homoleptic trigonal-bipyramidal Rh/Sn complexes have been reported, although accounts of studies on the structurally similar $[\text{Rh}(\text{SnCl}_3)_4\text{SnCl}_4]^{5-}$ and $\text{Pt}(\text{SnCl}_3)_5^{3-}$ have appeared in the literature.^{14,15}

In summary, the cyclic stannylene **1** seems to be a highly useful ligand in its ability to stabilize low-valent metal complexes. The facile replacement of PPh_3 by **1** is particularly noteworthy, since SnCl_2 apparently does not react with $\text{RhCl}(\text{PPh}_3)_3$ at all.¹⁶ Platinum-metal/tin(II) chloride mixtures are known to be useful catalysts for a number of industrial processes,¹⁷ and our efforts toward understanding the bonding in these interesting complexes and their chemical behavior are continuing.

Acknowledgment. L.S. thanks the Deutsche Forschungsgemeinschaft (DFG) for a stipend.

Supplementary Material Available: An Experimental Section, ORTEP drawings and complete atomic numbering schemes for **2**-toluene and **3**-toluene, and tables of crystallographic parameters, final positional and anisotropic thermal parameters for non-hydrogen atoms, isotropic thermal parameters, bond lengths, and bond angles for the two structures (16 pages); tables of observed and calculated structure factors (36 pages). Ordering information is given on any current masthead page.

- (13) See references cited in ref 12b and 15.
 (14) Kimura, T.; Sakurai, T. *J. Solid State Chem.* **1980**, *34*, 369.
 (15) Nelson, J. H.; Alcock, N. W. *Inorg. Chem.* **1982**, *21*, 1196.
 (16) Chan, D. M. T.; Marder, T. B. *Angew. Chem., Int. Ed. Engl.* **1988**, *27*, 442.
 (17) (a) Anderson, G. K.; Clark, H. C.; Davis, J. A. *Inorg. Chem.* **1983**, *22*, 427. (b) Anderson, G. K.; Clark, H. C.; Davies, J. A. *Ibid.* **1983**, *22*, 434.

Institute for Inorganic Chemistry
 Saarbrücken University
 D-6600 Saarbrücken, West Germany

Michael Veith*
 Lothar Stahl
 Volker Huch

Received March 15, 1989

Synthesis, Structure, and Reactivity of Cerium(III) Alkoxides. 2. Thermal Decomposition of $\text{Ce}(\text{OC}^t\text{Bu}_3)_3$ and the Structure of $[\text{Ce}(\text{OCH}^t\text{Bu}_2)_3]_2$

Well-characterized homoleptic metal alkoxides are of considerable interest as precursors to metal oxides. Both thermolytic and hydrolytic methods have been employed to convert alkoxides to the corresponding oxides.¹ Little, however, is known concerning the mechanistic steps involved in the thermal decomposition of metal alkoxides, especially those that lack accessible β -hydrogen atoms.² This contrasts with extensive mechanistic information available for the decomposition of the corresponding metal alkyl

- (1) Recent reviews: (a) Brinker, C. J.; Clark, D. E.; Ulrich, D. R. *Better Ceramics Through Chemistry II. Mater. Res. Soc. Symp. Proc.* **1986**, *73*. (b) *Science of Ceramic Chemical Processing*; Hench, L. L., Ulrich, D. R., Eds.; Wiley: New York, 1986. (c) *Ultrastructure Processing of Ceramics, Glasses and Composites*; Hench, L. L., Ulrich, D. R., Eds.; Wiley: New York, 1984. (d) Mazdiyasi, K. S. *Chem. Int.* **1982**, *8*, 42.
 (2) (a) Reference 1d. (b) Bryndza, H. E.; Tam, W. *Chem. Rev.* **1988**, *88*, 1163. (c) Bradley, D. C.; Mehrotra, R. C.; Gaur, D. P. *Metal Alkoxides*; Academic: New York, 1978. (d) Zook, H. D.; March, J.; Smith, D. F. *J. Am. Chem. Soc.* **1959**, *81*, 1617.

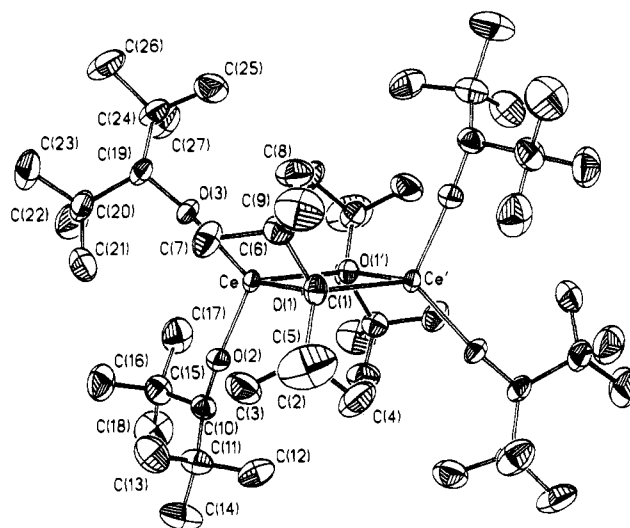


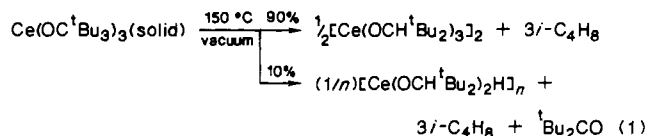
Figure 1. The molecular structure of **3** drawn with 40% probability thermal ellipsoids. Distances: Ce-O(1), 2.363 (3) Å; Ce-O(2), 2.142 (2) Å; Ce-O(3), 2.152 (3) Å. Angles: O(1)-Ce-O(1'), 74.3 (1)°; O(1)-Ce-O(2), 115.4 (1)°; O(1)-Ce-O(3), 114.0 (1)°; O(2)-Ce-O(3), 113.3 (1)°; O(2)-Ce-O(1'), 107.8 (1)°; O(3)-Ce-O(1'), 126.7 (1)°; Ce-O(1)-Ce', 105.7 (1)°.

species.³ Herein, we report the preliminary results of our study of the thermal decomposition of $\text{Ce}(\text{OC}^t\text{Bu}_3)_3$ (**1**) and the related $[\text{LiOC}^t\text{Bu}_3]_n$ (**2**) to the corresponding $\text{M}(\text{OCH}^t\text{Bu}_2)_n$ derivatives ($\text{M} = \text{Ce}, \text{Li}$).⁴ Our study provides a glimpse of the nucleation process that occurs during the formation of a metal oxide from the corresponding alkoxide through the loss of hydrocarbon fragments.

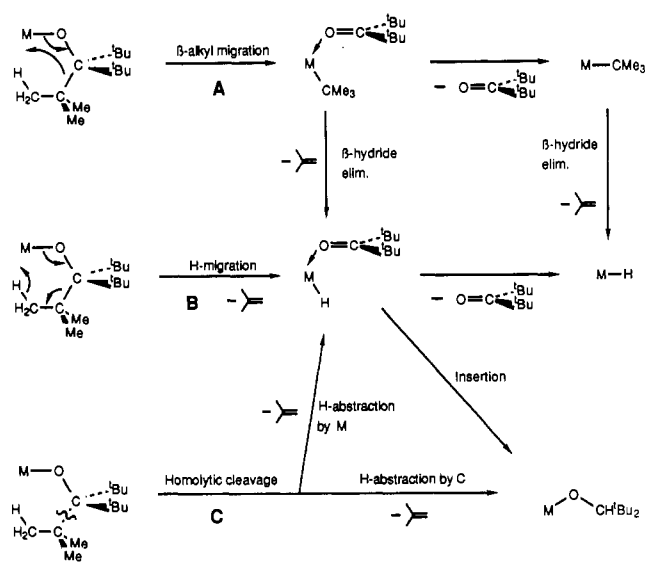
$\text{Ce}(\text{OC}^t\text{Bu}_3)_3$ (**1**) was synthesized by the reaction of $\text{Ce}[\text{N}(\text{SiMe}_2)_2]_3$ with HOCH^tBu_3 in pentane, and was isolated as an O_2 - and H_2O -sensitive yellow solid. **1** is monomeric in solution, and although its crystal structure has not been determined, it is safe to assume that it is also monomeric in the solid state. We have previously shown that the compound $\text{Ce}(2,6\text{-}^t\text{Bu}_2\text{-C}_6\text{H}_3\text{O})_3$ is monomeric in the solid state,⁵ and models indicate that OC^tBu_3 is significantly more bulky than $2,6\text{-}^t\text{Bu}_2\text{-C}_6\text{H}_3\text{O}$.

The lithium analogue, **2**, was obtained from $^t\text{Bu}_3\text{COH}$ and $^n\text{BuLi}$ in alkane solvent. It was assumed to be oligomeric based on the fact that the THF complex $[(^t\text{Bu}_3\text{CO})\text{Li}(\mu\text{-THF})]_2$, was shown to be a dimer in the solid state.^{4b}

Thermolysis of solid **1** at 150 °C under vacuum resulted in its decomposition to $[\text{Ce}(\text{OCH}^t\text{Bu}_2)_3]_2$ (**3**)⁶ and isobutylene. In addition, a small quantity of $^t\text{Bu}_2\text{CO}$ was detected, indicating the formation of a cerium(III) hydride. These results are summarized in eq 1. Hydrolysis of a C_6D_6 solution of the solid residue left



- (3) Recent reviews: (a) Crabtree, R. H. *The Organometallic Chemistry of the Transition Metals*; Wiley: New York, 1988; p 39. (b) Collman, J. P.; Hegedus, L. S.; Norton, J. R.; Finke, R. G. *Principles and Applications of Organotransition Metal Chemistry*; University Science Books: Mill Valley, CA, 1987; p 94.
 (4) While a similar reaction was reported for a bimetallic system, the mechanism of decomposition was not examined; see: (a) Hvoslaf, J.; Hope, H.; Murray, B. D.; Power, P. P. *J. Chem. Soc., Chem. Commun.* **1983**, 1438. (b) Murray, B. D.; Hope, H.; Power, P. P. *J. Am. Chem. Soc.* **1985**, *107*, 169.
 (5) Stecher, H. A.; Sen, A.; Rheingold, A. L. *Inorg. Chem.* **1987**, *27*, 1130.
 (6) ^1H NMR (C_6D_6) (25 °C) (ppm): 31.5 (br, terminal OCH^tBu_2); 7.0 (br, terminal OCH^tBu_2); -18.0 (br, bridging OCH^tBu_2). The resonance due to bridging OCH^tBu_2 could not be located. The broadness of the spectrum was due to the paramagnetic Ce(III) ion. This compound was also independently synthesized by the reaction of $\text{Ce}[\text{N}(\text{SiMe}_2)_2]_3$ with 3 equiv of HOCH^tBu_2 in pentane.

Scheme I. Possible Decomposition Pathways for $M(OC^tBu)_3$ 

after decomposition gave $HOCH^tBu_2$ as the only organic product (>99%).

The absence of structurally characterized dimeric lanthanide alkoxides⁷ prompted us to determine the crystal structure of **3** by single-crystal X-ray diffraction.⁸ As Figure 1 indicates, **3** is a dimer with a pseudotetrahedral geometry about each Ce atom. A crystallographic inversion center constrains the Ce and the bridging O atoms to a single plane, and a dihedral angle of 84.1° relates this plane to the O(terminal)-Ce-O(terminal) plane.

Scheme I outlines the plausible mechanistic pathways for the thermolysis and encompasses three rate-limiting decomposition modes (steps A–C). The H-migration pathways (step B) was judged to make a minor contribution at best, based on a k_H/k_D value of 1.5 observed for isobutylene in the decomposition of $Ce[OC(^tBu)(^tBu-d_9)_2]_3$.⁹ The corresponding k_H/k_D value for $\{Li[OC(^tBu)(^tBu-d_9)_2]\}_n$, which decomposed in an analogous fashion in the solid state, was 1.8.⁹

It is harder to differentiate between the β -alkyl migration and homolytic cleavage pathways (steps A and C, respectively). The C–C bonds between the quaternary carbons of the OC^tBu_3 ligand in metal complexes^{4a,b,10} as well as other tri-*tert*-butylmethyl systems¹¹ are relatively long (1.60–1.66 Å) and, therefore, are

relatively weak,¹² but this would favor both steps A and C. However, the following experimental results are more consistent with homolysis of the C–C bond (step C).

Thermolyses of **1**, **2**, and tBu_3COH were carried out in either benzene or toluene. While no detailed kinetic analysis was performed, the following are the approximate half-life ($t_{1/2}$) values obtained:¹³ $[LiOC(^tBu)_3]_n$, 80 min at $95^\circ C$; $Ce(OC^tBu)_3$, 60 h at $95^\circ C$; $HOCH^tBu_3$, 150 h at $140^\circ C$. Since free radicals are electron-deficient species, increased negative charge on the neighboring oxygen atom, which can be donated to the carbon participating in bond homolysis, should facilitate this process. The ionic nature of the OC^tBu_3 group would be expected to increase on going from the alcohol to the Ce compound to the Li compound, and hence, the trend in the homolysis rate would appear to be consistent with step C (although not necessarily inconsistent with step A). The addition of slightly less than 1 equiv of 12-crown-4 (which is known to complex strongly with Li^+ ¹⁴) to **2** prior to thermolysis resulted in a reduction of the half-life to under 1 min at $95^\circ C$.¹⁵ This is consistent with step C since the complexation of Li^+ by 12-crown-4 would lead to increased charge separation and, therefore, more negative charge on the oxygen of OC^tBu_3 . However, it is inconsistent with step A since distancing the metal from the OC^tBu_3 moiety should lead to a decrease in β -alkyl migration rate. The observation is also inconsistent with step B for a similar reason.

An experiment was performed to trap the $^tBu^*$ radical formed from the OC^tBu_3 ligand during thermolysis. Earlier 1H NMR titrations had shown that Ph_2CO forms a 1:1 complex with the Ce center in **1**.¹⁶ When a benzene solution of **1** was thermolyzed in the presence of 11 equiv of Ph_2CO , only a small fraction of the expected isobutylene was observed. When the reaction mixture was hydrolyzed, the nonvolatile organic products observed were Ph_2^tBuCOH , Ph_2CHOH , and tBu_2CO , along with excess Ph_2CO and $HOCH^tBu_3$. Significantly, no $HOCH^tBu_2$ was found. The first product was clearly formed by trapping of the $^tBu^*$ radical by coordinated Ph_2CO . The absence of $HOCH^tBu_2$ indicated that (a) the above trapping process was faster than H abstraction by the Ce- $OC^tBu_2^*$ fragment and/or (b) the larger tBu_2CO ligand was rapidly displaced by the smaller Ph_2CO from the Ce-(H)(tBu_2CO) intermediate, resulting in the eventual formation of the $CeOCHPh_2$ moiety rather than the $CeOCH^tBu_2$ moiety.

In conclusion, our results provide a mechanistic description of the pathways involved in the thermal decomposition of a metal alkoxide lacking accessible β -hydrogens.

Acknowledgment. A.S. acknowledges the support of this research by the donors of the Petroleum Research Fund, administered by the American Chemical Society. We also thank Professors L. M. Jackman and H. G. Richey for helpful discussions.

- (7) Structurally characterized monomeric lanthanide complexes: (a) Reference 5. (b) Hitchcock, P. B.; Lappert, M. F.; Singh, A. *J. Chem. Soc., Chem. Commun.* **1983**, 1499. (c) Hitchcock, P. B.; Lappert, M. F.; Smith, R. G. *Inorg. Chim. Acta* **1987**, *139*, 183.
- (8) Crystal data for **3**, $C_{24}H_{114}O_6Ce_2$ (obtained by recrystallization from toluene): triclinic, $P1$, $a = 11.611$ (7) Å, $b = 12.497$ (6) Å, $c = 12.611$ (7) Å, $\alpha = 63.78$ (4)°, $\beta = 70.69$ (4)°, $\gamma = 79.36$ (4)°, $V = 1542$ (1) Å³, $Z = 1$, $\mu = 15.03$ cm⁻¹, $D(\text{calc}) = 1.22$ g cm⁻³, $Mo K\alpha$ ($\lambda = 0.71073$ Å), $23^\circ C$, Nicolet R3m/ μ diffractometer. Of 5679 reflections collected ($4^\circ \leq 2\theta \leq 50^\circ$), 5409 were unique ($R(\text{int}) = 2.24\%$) and 4650 were observed ($F_o \geq 5\sigma(F_o)$). An empirical absorption correction was applied ($T_{\text{max}} = 0.744$; $T_{\text{min}} = 0.654$). A Patterson map located the Ce atom, non-hydrogen atoms were refined anisotropic, and H atoms were refined isotropic (calculated, $d(C-H) = 0.960$ Å): $R_F = 2.87\%$, $R_wF = 3.12\%$, data/parameter = 16.6, GOF = 0.913, highest peak = 0.81 e/Å³ (Ce noise). All software: Shelldrick, G. "SHELXTL (5.1)"; Nicolet XRD; Madison, WI.
- (9) The decomposition was carried out under vacuum at $150^\circ C$ for 3 h. Kinetic isotope effects were calculated from intensity of d_0 vs d_9 isobutylene ($m/e = 56$ and 64) and d_9 vs d_{18} tBu_2CO ($m/e = 151$ and 160), correcting for the 2:1 statistical preference for the heavier group. For **1**, isobutylene gave 1.50 and tBu_2CO gave 1.23; for **2**, isobutylene gave 1.84 and tBu_2CO gave 1.49. At present, we are unable to explain why the ketone-derived value is lower; we believe it suggests that the formation of tBu_2CO occurs after isobutylene formation with its own independent rate-limiting step and k_H/k_D .
- (10) (a) Lubben, T. V.; Wolczanski, P. T. *J. Am. Chem. Soc.* **1987**, *109*, 424. (b) Lubben, T. V.; Wolczanski, P. T.; Van Duynne, G. D. *Organometallics* **1984**, *3*, 977. (c) Murray, B. D.; Power, P. P. *J. Am. Chem. Soc.* **1984**, *106*, 7011. (d) Olmstead, M. M.; Power, P. P.; Sigel, G. *Inorg. Chem.* **1986**, *25*, 1027. (e) Stecher, H. A.; Sen A.; Rheingold, A. L. Manuscript in preparation.

- (11) (a) Cheng, P.-T.; Nyburg, S. C.; Thankachan, C.; Tidwell, T. T. *Angew. Chem., Int. Ed. Engl.* **1977**, *16*, 654. (b) Cheng, P.-T.; Nyburg, S. C. *Acta Crystallogr., B* **1978**, *B34*, 3001. (c) Hagler, A. T.; Stern, P. S.; Lifson, S.; Ariel, S. *J. Am. Chem. Soc.* **1979**, *101*, 813. (d) Ruchardt, C.; Weiner, S. *Tetrahedron Lett.* **1979**, 1311. (e) Wong-Ng, W.; Chen, P.-T.; Nyburg, S. C. *Acta Crystallogr., C* **1984**, *C40*, 92.
- (12) Previous experimental and theoretical results on the thermolysis of bulky hydrocarbons indicated that the activation energy for C–C bond cleavage was inversely proportional to the ground-state strain enthalpy which in turn directly correlated with the C–C bond length, see: Ruchardt, C.; Beckhaus, H.-D. *Angew. Chem., Int. Ed. Engl.* **1980**, *19*, 429.
- (13) The decompositions of **2** and tBu_3COH were followed by 1H NMR spectroscopy. The decomposition of **1** in solution was not as clean as in the solid state, perhaps due to further reactions of the unstable intermediates. Hence, the reaction was followed by hydrolyzing aliquots removed from the reaction mixture and monitoring the amount of tBu_3COH presently by GC.
- (14) Pacey, G. E. In *Lithium, Current Applications in Science, Medicine, and Technology*; Bach, R. O., Ed.; Wiley: New York, 1985; p 35.
- (15) In the presence of 12-crown-4, isobutane rather than isobutylene was the predominant product, and in addition, a significant amount of tBu_2CO was formed. We attribute the change in product distribution to 12-crown-4 acting as a good hydrogen donor for the $^tBu^*$ radical. In support of this assumption, we observed extensive degradation of the crown ether in the course of the reaction.
- (16) For a description of a similar titration, see ref 5.

Supplementary Material Available: Tables of atomic coordinates, bond lengths, bond angles, anisotropic thermal parameters, H atom coordinates, and isotropic thermal parameters (5 pages); a table of observed and calculated structure factors (28 pages). Ordering information is given on any current masthead page.

Department of Chemistry
The Pennsylvania State University
University Park, Pennsylvania 16802

Hilmar A. Stecher
Ayusman Sen*

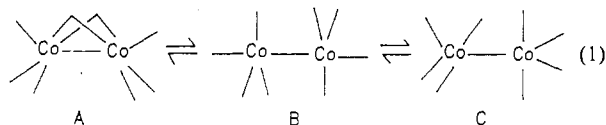
Department of Chemistry
University of Delaware
Newark, Delaware 19716

Arnold L. Rheingold*

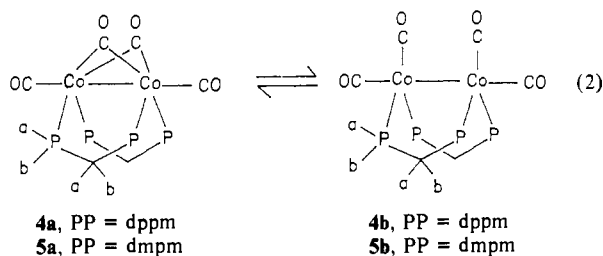
Received April 18, 1989

Thermodynamics and Dynamics of the Equilibrium between Carbonyl-Bridged and Nonbridged Isomers of $[\text{Co}_2(\text{CO})_4(\mu\text{-R}_2\text{PCH}_2\text{PR}_2)_2]$ (R = Me, Ph)

The complex $[\text{Co}_2(\text{CO})_8]$ and its phosphine-substituted derivatives are important in catalysis, and the interconversion between its three structural forms, A-C, has been studied in detail (eq 1).¹⁻⁴



However, the interconversions are too rapid even at -150°C to allow a study of the dynamics by ^{13}C NMR spectroscopy, and so little is known about the fluxionality.³ The situation is similar in those phosphine-substituted derivatives that have been studied previously, including $[\text{Co}_2(\text{CO})_4(\mu\text{-CO})_2(\mu\text{-dppm})]$.⁵ It is therefore of interest that the complexes $[\text{Co}_2(\text{CO})_4(\mu\text{-dppm})_2]$ (**4**)^{6,7} and $[\text{Co}_2(\text{CO})_4(\mu\text{-dmpm})_2]$ (**5**)⁸ (dppm = $\text{Ph}_2\text{PCH}_2\text{PPh}_2$, dmpm = $\text{Me}_2\text{PCH}_2\text{PMe}_2$) can exist in either bridged or unbridged forms (eq 2) and that the dynamics of the reaction can be studied by NMR spectroscopy.



The equilibria were most readily monitored by variable temperature FTIR spectroscopy (Figure 1, supplementary material).

Table I. Thermodynamic and Kinetic Data for the Carbonyl-Bridged \rightleftharpoons Nonbridged Isomerism

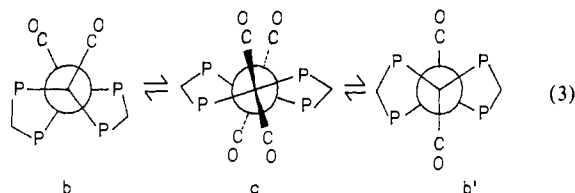
complex	$\Delta H/\text{kJ mol}^{-1}$	$\Delta S/\text{J K}^{-1} \text{mol}^{-1}$	ratio b:nb ^c		$\Delta G^\ddagger/\text{kJ mol}^{-1}$
			298 K	190 K	
$[\text{Co}_2(\text{CO})_8]^a$	+5.6	+21	44:56	74:26	27
$[\text{Co}_2(\text{CO})_4(\mu\text{-dppm})_2]^b$	+22.1 (1.5)	+102 (8)	3:97	85:15	41.5 (1.0)
$[\text{Co}_2(\text{CO})_4(\mu\text{-dmpm})_2]^b$	+26.3 (2.1)	+107 (13)	9:91	98:2	47 (1)

^a For A \rightleftharpoons B in pentane or hexane (eq 1) from ref 2 and 3. The value for ΔG^\ddagger was obtained in a hexane matrix and assumes no matrix contribution. This is reasonable in light of recent work.¹³ ^b For a \rightleftharpoons b in CH_2Cl_2 (eq 2). ^c b = CO bridged form, and nb = nonbridged form; these ratios are the calculated values at 298 or 190 K based on the ΔH and ΔS values given.

This showed clearly that the unbridged isomer **4b** or **5b** was favored at higher temperatures and the bridged form **4a** or **5a** was favored at lower temperatures.⁹ The equilibrium constants were determined over a range of temperatures from 190 to 301 K, and the thermodynamic data were then determined (Table I).¹⁰ In each case, the enthalpy term strongly favors the carbonyl-bridged form while the entropy term strongly favors the unbridged form. The effect is much greater than in $[\text{Co}_2(\text{CO})_8]$ ¹⁻⁴ as can be seen from the data in Table I.

The fluxionality of **4** and **5** was studied by ^1H , ^{13}C , and ^{31}P NMR spectroscopies, with the ^{13}C NMR spectra obtained on ^{13}C CO-enriched samples.¹¹ For example, the ^{13}C NMR spectrum of **4** at low temperature gave two carbonyl resonances due to **4a** and one due to **4b**, and the resonances coalesced to give a singlet at room temperature (Figure 2, supplementary material). Similarly, the ^1H NMR spectrum due to the CH_2P_2 protons gave a singlet at room temperature but gave two broad resonances for **4a**, due to the nonequivalent protons CH^aH^b , and one resonance for **4b** at low temperature. A single ^{31}P resonance was observed at room temperature but two resonances, one for each of **4a** and **4b**, were observed at low temperatures (Figure 2). Very similar spectroscopic features were observed for complex **5**, and this complex also gave two resonances due to the nonequivalent Me^aP and Me^bP groups of **5a** at low temperature, but gave a single resonance at room temperature.

It is clear that **4b** or **5b**, in the static form established crystallographically for the solid state of **4b**, should also give two carbonyl resonances and two $\text{CH}^a\text{H}^b\text{P}_2$ resonances, but this nonequivalence was not observed. Furthermore, the reaction of eq 2 does not, of itself, lead to equivalence of the carbonyl groups or the CH^aH^b protons of **4a** or **5a**. Thus, a second form of fluxionality with a much lower activation energy must occur within the nonbridged form **4b** or **5b**. The mechanism of eq 3 (showing



Newman projections along the Co-Co bond), involving reversible reaction of $b \rightleftharpoons c$ is most reasonable,¹⁻⁴ since c is analogous to

- (1) Bor, G.; Dietler, U. K.; Noack, K. *J. Chem. Soc., Chem. Commun.* 1976, 914.
- (2) Noack, K. *Helv. Chim. Acta* 1964, 47, 1064.
- (3) Lichtenberger, D. L.; Brown, T. L. *Inorg. Chem.* 1978, 17, 1381.
- (4) Sweany, R. L.; Brown, T. L. *Inorg. Chem.* 1977, 16, 415.
- (5) Onaka, S.; Shriver, D. F. *Inorg. Chem.* 1976, 15, 915.
- (6) Liscic, E. C.; Hanson, B. E. *Inorg. Chem.* 1986, 25, 812.
- (7) Elliot, D. J.; Holah, D. G.; Hughes, A. N. *Inorg. Chim. Acta* 1988, 142, 195.
- (8) The complexes **4a** and **4b** have been characterized by X-ray structure determinations. Elliot, D. J.; Holah, D. G.; Hughes, A. N.; Magnuson, V. R.; Moser, I. To be submitted for publication.
- (9) The complex **5** was prepared by reaction of cobalt(II) bromide with $\text{Na}[\text{BH}_4]$ in the presence of CO and the diphosphine ligand.

(9) FTIR data [$\nu(\text{CO})/\text{cm}^{-1}$ in CH_2Cl_2]: **4a**, 1951, 1924, 1765 sh, 1753; **4b**, 1972, 1953, 1921; **5a**, 1945, 1916, 1735 sh, 1716; **5b**, 1953, 1920, 1893. The observation of nearly isosbestic points in each case indicates that only two isomers are present.

(10) In each case data were measured at two wavelengths, and the data given are the mean values determined.

(11) NMR data at low temperature in CD_2Cl_2 are as follows. **4a**: ^1H , -90°C , $\delta = 2.84, 3.71$ (CH^aH^b); ^{13}C , -70°C , $\delta = 206.0$ (terminal CO), 244.3 ($\mu\text{-CO}$); ^{31}P , -70°C , $\delta = 44.8$. **4b**: ^1H , -90°C , $\delta = 3.89$ (CH_2); ^{13}C , -70°C , $\delta = 213.95$ (CO); ^{31}P , -70°C , $\delta = 37.4$. **5a**: ^1H , -92°C , 1.93, 2.75 (CH^aH^b), 1.50 (MeP); ^{13}C , -82°C , $\delta = 203.5$ (terminal CO), 265.5 ($\mu\text{-CO}$), $\delta = 19.5, 19.0$ (MeP); ^{31}P , -62°C , $\delta = 29.85$. **5b**: ^1H , -90°C , $\delta = 2.19$ (CH_2), 1.34 (MeP); ^{13}C , not resolved; ^{31}P , -62°C , $\delta = 19.3$. The chemical shifts and peak widths were, in many cases, temperature dependent, at least partly due to the quadrupole of cobalt (see Figure 2).